CHAPTER THREE

MATERIALS AND METHODS

3.0 Introduction

This chapter presents the materials, chemicals and methods employed in this research work. It is presented in sections and subsections which include list of chemicals and suppliers, analytical methods and hydrodeoxygenation reactor. Others include catalyst preparation via incorporation of different metal-oxide and metal-oxalate precursors, catalyst characterization, catalyst testing, optimization, kinetic studies and process modeling in Aspen Hysys process simulator v7.2 (AHPS).

3.1 Chemicals and Materials

3.1.1 Chemicals

The 3 dimensional structures of the two selected bio-oil model compounds in this study are shown in Figures 3.1 and 3.2; their detail information generated from AHPS is located in Appendix A1 – A2. The list of chemicals and materials, their suppliers and application are presented in Table 3.1.

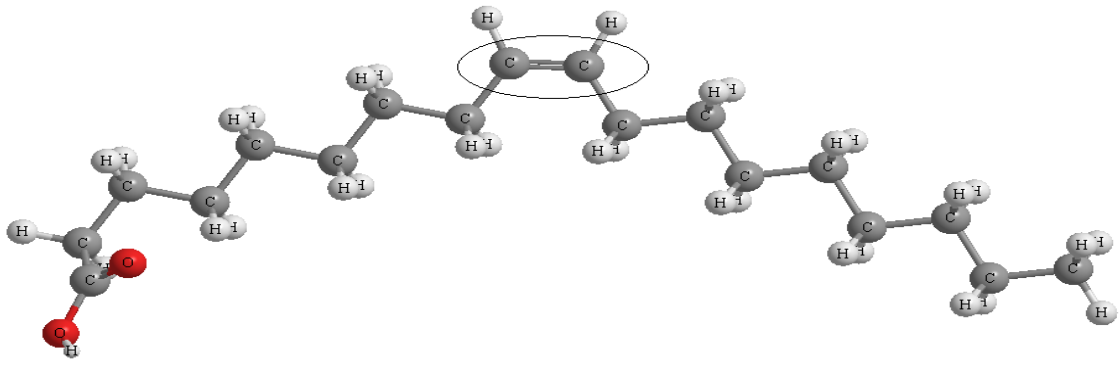

Figure 3.1 Structure of oleic acid (ring showing presence of double bond)

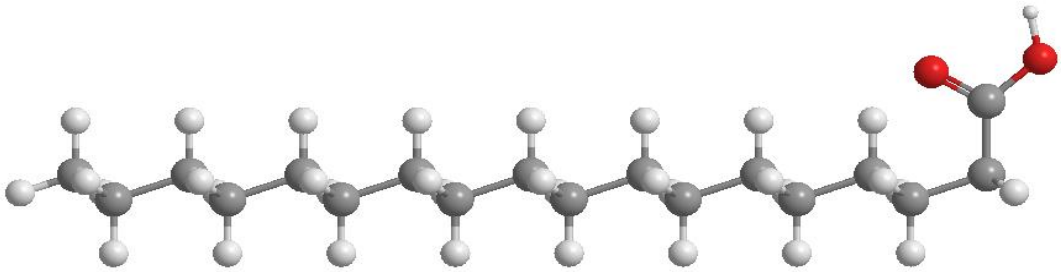

Figure 3.2 Structure of stearic acid (no double bond)

Table 3.1 List of chemicals and materials

Chemical/material	Specification	Supplier	Usage
Hydrofluoric acid	68%	Merck, Germany	pH control
Oxalic acid	Anhydrous	Sigma-Aldrich	Catalyst precursor preparation
Alumina	Powder	F.S. Chemicals	Catalyst support
Zeolite A (99%)	Powder	F.S. Chemicals	Catalyst support
Bis(acetylacetonato)dioxomolybdenum(VI)	Yellowish Powder	Sigma-Aldrich	Catalyst precursor
Dihidrogen palladium hexahydrate	Brownish powder	Sigma-Aldrich	Catalyst precursor
Nickel nitrate hexahydrate	Green hydrated solid	Sigma-Aldrich	Catalyst precursor
Potassium hexachloroplatinate	Brownish powder	Merck, Germany	Catalyst precursor
GC-MS vial	Small blue capped bottles	Sigma-Aldrich, Malaysia	Biofuel sampling
Oleic acid (99%)	Viscous oil	Sigma-Aldrich, Malaysia	Bio-oil
Stearic acid (99%)	Semi solid	Sigma-Aldrich, Malaysia	Bio-oil

3.2 Thermodynamic Process Simulation for the Hydrodeoxygenation Feasibility Studies

As earlier identified in the literature survey that oleic acid (OA) and stearic acid (SA) are the most common fatty acids found in virtually all known natural occurring triglycerides such as coconut oil, palm kernel oil, palm oil, olive oil, in fact they seldom has the highest percentage. For example, in Shea butter which hitherto has not been considered as a veritable feed stock for the production of biofuel, OA and SA respectively have 49% and 41% mass compositions (www.sheabutteruganda.com, March 2014). Consequently, both OA and SA are considered for simulation in this study more so that they also represent unsaturated and saturated fatty acid, respectively.

3.2.1 Process Chemistry

The thermodynamic feasibility of the hydrodeoxygenation (HDO) of the model compounds' (MCs) process chemistry was established in a conversion reactor using AHPS based on the proposed Equation 3.1 and 3.2, for OA ($C_{17}H_{33}COOH$) and SA ($C_{17}H_{35}COOH$), respectively and the best operating conditions were determined through rigorous thermodynamic simulation.

$$C_{17}H_{33}COOH + 4H_2 \rightarrow C_{18}H_{38} + 2H_2O \quad (3.1)$$

$$C_{17}H_{35}COOH + 3H_2 \rightarrow C_{18}H_{38} + 2H_2O \quad (3.2)$$

3.2.2 Simulation Basis Manager (SBM)

The SBM environment was built following standard procedure of Apsen Technology Inc. manual described by Santana et al. (2010). The components in

the proposed chemistry for the HDO process of the MCs were selected from AHPS Component Library. The thermodynamic, transport and other properties information about the components and process products (OA, SA, H_2, H_2O, CO and CO_2) were found in the simulator component library. The non-random two liquid (NRTL) thermodynamic fluid package was chosen as the prefered package for calculation of activity coefficient due to the presence of CO and H_2O which are not just oxygenated compounds but also polar. The unavailable binary interaction parameters in the simulation databank were estimated using the UNIFAC vapor–liquid equilibrium and UNIFAC liquid–liquid equilibrium methods (Santana et al., 2010). On the reaction page, the reactants were assigned a negative sign along their coefficients while the products were assigned positive. The desired extent of reaction was specified and the reaction sets were attached to the earlier selected NRTL fluid package.

3.2.3 Simulation Basis Environment and Process Description

In the simulation basis environment that comprises both the Process Flow Diagram (PFD) and Workbook, each of the components were built into the Workbook and assigned a Stream name as seen on the PFD (Figure 3.3). The conversion reactor was installed on the PFD and the neccesary Streams were attached. The result of simulation on reaction temperature and pressure and reactants (stoichiometry) flow rates were monitored using the AHPS Databook facilities and plotted accordingly. The degree of conversion of MCs was monitored on OA and SA.

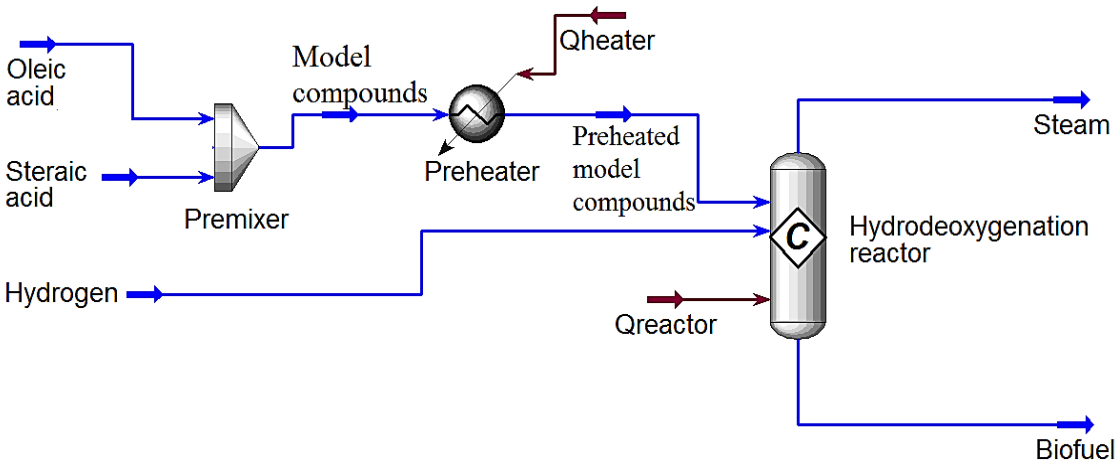

Figure 3.3 Simplified Process Flow Diagram for the hydrodeoxygenation of model compounds

3.3 Catalyst Development

In this study, seven different types of catalyst were prepared using different metals and preparation protocols with each new synthesis procedure as an improvement over the previous ones. Firstly, in view of the contemporary growing interest in organometallic catalysis, metal-oxide and metal-oxalate supported catalysts were synthesized using nickel as the active metal. Their activities were compared and the nickel-oxalate showed superiority to nickel oxide. The choice of nickel for this comparison was based on its relatively low cost compared to other active metals such as palladium and platinum also used in this report. Furthermore, in order to enhance the isomerization activity of the synthesized catalysts, fluoride ion functionalized palladium-oxalate catalyst with increased acidity was synthesized and its activity was compared with a non-fluoride ion functionalized palladium-oxalate catalyst. In view of the exceptional invaluable enhanced HDO and isomerization activity of the synthesized -fluoride ion functionalized palladium-oxalate catalyst, different metals such as molybdenum and platinum were functionalized accordingly and their activities were

compared. The last catalyst investigates the applicability of bi-metallic catalyst using molybdenum to promote nickel supported on zeolite catalyst.

3.3.1 Preparation of Nickel Oxalate ($NiOx/Al_2O_3$) and Nickel Oxide (Ni/Al_2O_3) Alumina Supported Catalysts

Nickel oxalate catalyst was prepared via functionalization of 18.84 g nickel nitrate with equimolar oxalic acid (OxA) to yield the polynulcear nickel II oxalate complex (NiOx) in an aluminum foil wrapped conical flask (Plate 3.1) due to the high photo sensitivity index of metal oxalate ligands (Ayodele, 2013). The NiOx was subsequently incorporated into 50 g alumina dispersion using simple dissolution method. The inorganic nickel supported on alumina catalyst (Ni/Al_2O_3) was prepared by the same method but without OxA functionalization. Both Ni/Al_2O_3 and the nickel oxalate alumina supported ($NiOx/Al_2O_3$) catalysts were filtered and dried in the oven at 100 ºC, grinded and calcined at 400 ºC for 4 h followed by characterization and testing.

Plate 3.1 Aluminum foil wrapped conical flask due to the high photo sensitivity index of metal oxalate ligands

3.3.2 Preparation of palladium oxalate zeolite supported catalyst (PdOx/Zeol)

The HDO catalyst was synthesized via functionalization of 2.36 g of H_2PdCl_4 with stoichiometric ratio of aqueous OxA and was ripened for 1 h to develop the polynuclear palladium (II) oxalate complexes (PdOx) in an aluminum foil wrapped 500 ml conical flask because of the metal-oxalate complex photo-sensitivity (Ayodele, 2013). The precursor was then added to already prepared 50 g zeolite (Zeol) dispersion and left stirring for 4 h at 50 ºC for the deposition of PdOx particles on the Zeol support, the pH was observed to stabilize at 5.3 ± 0.3 as the stirring progressed. The synthesized palladium oxalate zeolite supported catalyst (PdOx/Zeol) was filtered and washed to remove the chloride ions followed by drying at 100 ºC for 12 h and calcined at 400 ºC for 3 h based on some few preliminary studies.

3.3.3 Preparation of fluoride ion modified palladium oxalate zeolite supported catalyst (FPdOx/Zeol)

The catalyst synthesis was achieved by reacting 2.36 g of H_2PdCl_4 with aqueous oxalic acid in stoichiometric ratio to yield the polynuclear palladium (II) oxalate complexes in a 500 ml conical flask wrapped aluminum foil since metal oxalate complexes have high photo-sensitivity index expecially under UV light (Ayodele and Togunwa, 2014). As the reaction proceeded, drops of 2 M HF acid were added to lower the pH from in situ 5.4 to 3.5 and the solution was ripened for 1 h, the resulting fluoro palladium oxalate (FPdOx) complex was carefully added to the already prepared 50 g of Zeol dispersion under intense stirring at 50 °C to ensure successful incorporation of the FPdOx into the Zeol matrix. The resulting product was filtered, washed with deionized water to remove chloride ions and dried in the oven at 110 °C. The synthesized fluoro-

palladium oxalate supported zeolite catalyst (FPdOx/Zeol) was finally grounded to powder and calcined at 400 °C for 3 h.

3.3.4 Preparation of fluoro-molybdenum-oxalate zeolite supported catalyst (FMoOx/Zeol)

The catalyst was developed by first synthesizing the molybdenum oxalate catalyst precursor from stoichiometric ratio of 6.81 g of bis(acetylacetonato)dioxo-molybdenum(VI) and oxalic acid (OxA) at 60 ºC in an aluminum foil wrapped conical flask because of metal oxalate high photo sensitivity index. As the reaction proceed drops of 4 M hydrofluoric acid were intermittently added until the pH was observed to decrease from the in situ 5.2 to 3.5 ± 0.3 (Kitano et al., 2013) (as monitored by EcoScan SC11-4115, Exatech Enterprise pH meter) to ensure the formation of the fluoro-molybdenum-oxalate (FMoOx) complex. The FMoOx was then added to 20 g zeolite (Zeol) dispersion under brisk stirring at 70 ºC for 4 h and allowed to age for 1 h, followed by filtration, washing and drying in the oven at 120 ºC for 12 h. The synthesized fluoro-molybdenum-oxalate zeolite supported catalyst (FMoOx/Zeol) was then grinded and calcined at 400 ºC for 3 h.

3.3.5 Preparation of fluoro-platinum-oxalate zeolite supported catalyst (FPtOx/Zeol)

The catalyst was developed by first synthesizing the platinum oxalate catalyst precursor from stoichiometric ratio of 2.48 g of K_2PtCl_4 and oxalic acid (OxA) at 60 ºC in an aluminum foil wrapped conical flask because of metal-oxalate high photo sensitivity index. As the reaction proceed drops of 4 M hydrofluoric acid were

intermittently added until the pH decrease from the in situ 5.7 to 3.5 ± 0.3 (Kitano et al., 2013) (as monitored by EcoScan SC11-4115, Exatech Enterprise pH meter) to ensure the formation of the fluoro- platinum -oxalate (FPtOx) complex . The FPtOx was then added to 20 g zeolite (Zeol) dispersion (in deionized water) under brisk stirring at 70 ºC for 4 h and allowed to age for 1 h, followed by filtration, washing and drying in the oven at 120 ºC for 12 h. The synthesized fluoro- platinum -oxalate zeolite supported catalyst (FPtOx/Zeol) was then grinded and calcined at 400 ºC for 3 h.

3.3.6 Preparation of molybdenum modified zeolite supported nickel fluorooxalate catalyst (NiMoFOx/Zeol)

The catalyst was prepared in a two-step technique viz: support preparation and catalyst precursor preparation and incorporation. In the first step, molybdenum oxalate freshly prepared by reacting stoichiometric ratio (1:1) of 8.32 g of bis(acetylacetonato)dioxo-molybdenum(VI) with oxalic acid in an aluminum foil wrapped conical flask because of metal oxalate high photo sensitivity index (Ayodele and Togunwa, 2014) was added to 50 g dispersion of zeolite and stir for 2 h at 50 ºC, followed by filtration, washing with distilled water and drying at 120 ºC for 12 h, then grinded into powder. In the second stage, 15.4 g of nickel nitrate hexahydrate was reacted with oxalic acid and drops of 4 M hydrofluoric acid were added intermittently to ensure the formation of the nickel fluorooxalate (NiFOx) complex. The pH was observed to reduce from in situ 5.48 until maintained at 2.5 ± 0.3 (as monitored by EcoScan SC11-4115 Exatech Enterprise pH meter) since previous study (Ng et al., 1985) has reported that the range of formation of metal-oxalate polymeric complex is 2.75 > pH >1.25. The NiFOx was then added to the molybdenum modified zeolite (MoOx/Zeol) dispersion under brisk stirring at 70 ºC for 4 h and allowed to age for 1 h,

followed by filtering, washing and drying in the oven at 120 ºC for 12 h. The synthesized molybdenum modified zeolite supported nickel fluorooxalate catalyst (NiMoFOx/Zeol) was then grinded and calcined for 4 h at 400 ºC.

3.4 Catalyst Characterization Techniques

The catalysts and their supports were characterized by Thermal gravimetric analysis (TGA), X-ray fluorescence spectroscopy (XRF), energy dispersive X-ray (EDX), scanning electron microscopy (SEM), X-ray diffraction (XRD), nitrogen adsorption/desorption isotherm (BET), Fourier transformed infrared spectroscopy (FTIR), and Raman spectroscopy techniques.

3.4.1 Thermal Gravimetric Analysis (TGA)

TGA analyses were carried out with a SHIMADZU DTG-60/60H instrument to determine the weight loss on the samples with temperature increment in order to determine the heat treatment required during calcination. 2 g of each sample was heated in a silica crucible at a constant heating rate of 10 ^{o}C/min operating in a stream of N_2 atmosphere with a flow rate of 40 mL/min from 25 to 700 ^{o}C and weight loss per time, weight loss per temperature increment and temperature increment versus time were recorded using a software installed on the computer attached to the TGA instrument.

3.4.2 X-ray Fluorescence (XRF)

XRF analyses of the samples were done using µXay µEDX 100 Schmadzu, NY and X-ray tube of rhodium anode and scintillation detector operating on a 40 mA

current and 40 mV voltage to determine the chemical composition and spectra of the sample. In order to achieve this, 4.0 g of each sample to be analyzed were pressed into a circular disc of 4 cm diameter and about 5 mm thickness using a manually operated hydraulic press. High-energy X-rays were used to bombard the circular discs to cause ionization of their component atoms; in this process, energy is released in the form of a photon which corresponds to the energy characteristics of the atom present. The X-ray reflections from the excited samples were detected by the scintillation detector which essentially consists of a 3-5 mm thick silicon junction type p-i-n diode with a bias of -1 kV across it. The detector was maintained at low temperature, and liquid-nitrogen was used to obtain the best resolution, the detected spectra were amplified and recorded using the computer program installed on the XRF analyzer.

3.4.3 Energy Dispersive X-ray (EDX)

This was performed to determine the elemental composition of the catalysts and their supports using EDX microanalysis system (Oxford INCA 400, Germany) connected to the SEM machine. The EDX analysis used Mn-Kα as the energy source operated at 15 kV of accelerating voltage, 155 eV resolutions and 22.4^{o} take off angle. The samples were analyzed three times and the average value was recorded. The results of analysis were presented in weight percent.

3.4.4 Scanning Electron Microscopy (SEM)

Scanning Electron Microscopy (SEM) was used to study the surface morphology of all the samples. The analysis was carried out using a scanning electron microscope (Model EMJEOL- JSM6301-F) with an Oxford INCA/ENERGY-350

microanalysis system. The samples were evenly distributed on a black double sided carbon tape attached to the aluminum stub and vacuumed for about 10 min prior to analysis. The samples were scanned at various magnifications.

3.4.5 Nitrogen Adsorption/Desorption Isotherm

Nitrogen adsorption–desorption measurements (BET method) were performed on the samples at liquid nitrogen temperature (−196 ^{o}C) with an autosorb BET apparatus, Micromeritics ASAP 2020 to determine the surface area, pore size/structure, and the pore volume. The analysis procedure is automated and operates with the static volumetric technique. Before each measurement, the samples were first degassed at 300 ^{o}C for 2 h and thereafter kept at liquid nitrogen temperature to adsorb nitrogen. The adsorption-desorption isotherm were obtained by measuring the equilibrium pressure during the adsorption and desorption of known volume of liquid nitrogen. The surface area, average pore size distribution and porosity of the samples were measured from the N_2 adsorption/desortion process and the values were calculated by Micropore version 2.46 software using Brunauer-Emmet-Teller (BET) equation to calculate specific surface area, while the total pore volume and average pore size distribution were calculated by t-plot method and Barrett-Joyner-Halenda (BJH) model, respectively.

3.4.6 X-ray Diffraction (XRD)

The X-ray diffraction (XRD) patterns of the catalysts and their supports were measured with Philip PW 1820 diffractometer to determine the crystal phase and structure of the metal oxides earlier detected by XRF and EDX analysis. Diffraction patterns of the samples were recorded with Cu Kα radiation and recorded in the range of

5-90^{o} (2 theta) with a scanning rate of 2^{o}/min and a step size of 0.01^{o}. The X-ray tube was operated at 40 kV and 120 mA.

3.4.7 Fourier Transformed Infrared Spectroscopy (FTIR)

Fourier transformed infrared spectroscopy analyses were performed on the samples to determine the functional groups present in order to understand the chemistry of the catalysts and their supports. The instrument used was Perkin-Elmer Spectrum GX Infrared Spectrometer with resolution of 4 cm^{-1} operating in the range of 4000-400 cm^{-1}. The samples and analytical grade KBr were dried at 100 ^{o}C over-night prior to the FTIR analysis. A mixture of 0.25 mg of each sample and 100 mg of KBr were grinded to fine particles and was placed in a manually operated hydraulic press operated at 8 Mbar to obtain a translucent disc of 12.7 mm diameter and about 1 mm thickness. The disc was securely placed in the disc holder and place in the analysis chamber. The spectra were automatically plotted by the software (Spectrum version 5.0.2) installed on the computer attached to the FTIR instrument.

3.4.8 Raman spectroscopy

The Raman spectroscopy was carried out to determine the type of interaction between the incorporated metal and the supports. The spectra were obtained with a Spex Triplemate spectrograph coupled to a Tracor Northern 1024 large area intensified diode array detector. The excitation source was a 488-nm line (Lexel Model No. 95 Ar^{+}) laser with a grating monochromator used to reject any spurious lines and background from the laser before the radiation entered the spectrometer. The spectra were taken with 1

cm^{-1} resolution. Signal averaging and spectral subtraction were used to improve the signal-to-noise ratio since the spectra are totally digital and no gratings were moved.

3.5 Catalytic Hydrodeoxygenation of Bio-Oil

3.5.1 Quantitative Hydrodeoxygenation (HDO) Experiments and product analysis

In order to understand the HDO process chemistry of the MCs and more especially to determine the activity and selectivity of the synthesized catalysts each of them (i.e. OA and SA) was hydrodeoxygenated individually. Their HDO was conducted in a 100 mL high pressure semi-batch reactor shown in Plate 3.2. The reaction temperature, pressure and gas flow rate (90 vol% N_2 and 10 vol% H_2) were varied within 320 - 380 °C, 20 – 60 bar and 50 – 150 mL/min, respectively based on preliminary studies. The flow of carrier gas and reaction pressure inlet and outlet were controlled by a flow (Brooks 58505 S) and a pressure controller (Brooks 5866), respectively. In a typical experiment, 40 g of OA or SA was added to the reactor followed by certain predetermined amount of catalyst and the catalyst was reduced in situ under flowing H_2 at 200 °C for 1 h prior to use after which the reactor was purged with He gas. The operating temperature was established and monitored by a type-K Omega thermocouple placed inside the reactor. Before the reaction started, a known gas flow rate (depending on the gas flow rate to be studied) was passed through the reactor to build reactor pressure to the desired pressure and the reaction commences by turning on the stirrer at an optimum speed of 2000 rpm (based on preliminary studies). Liquid samples withdrawn from the reactor were dissolved in pyridine and thereafter silylated with (100 wt% excess of) N,O-bis(trimethyl)-trifluoroacetamide, BSTFA in an oven at 60 °C for 1 h prior to GC analysis. The internal standard eicosane, $C_{20}H_{42}$ was added for

quantitative calculations. The withdrawn samples were analyzed with a gas chromatograph (GC, HP 6890) equipped with DB-5 column (60m x 0.32mm x 0.5 mm) and a flame ionization detector. 1 ml sample was injected into the GC with split ratio of 50:1 and helium was used as the carrier gas. The chromatographic pressure program was well-adjusted to achieve satisfactory separation of the desired product and the product identification was validated with a gas chromatograph–mass spectrometer (GC–MS) shown in Plate 3.3.

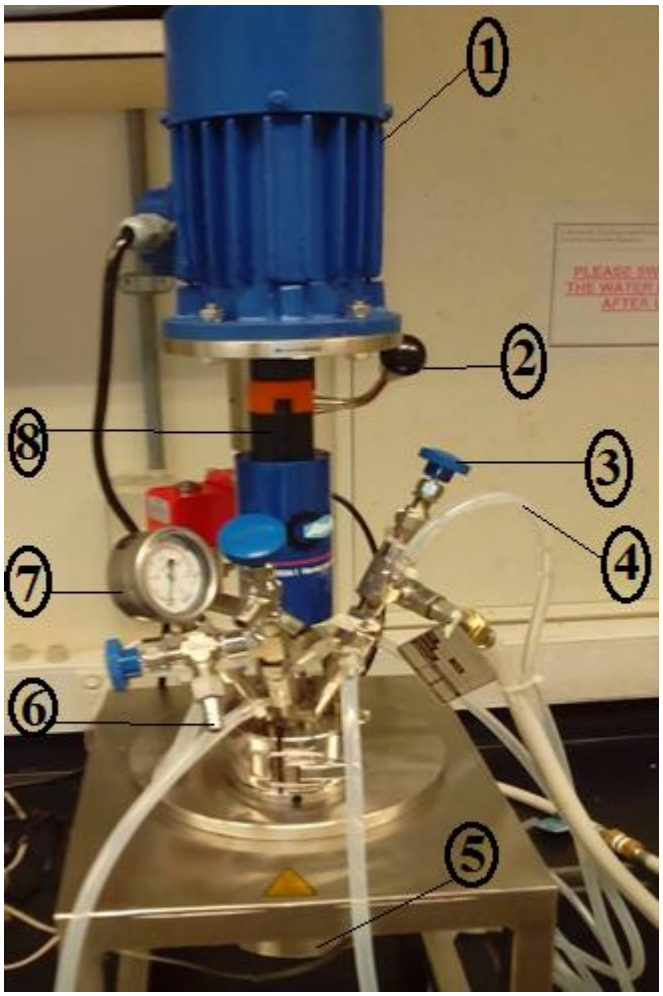

Plate 3.2 High pressure semi-batch reactor, (1) electric motor (2) electric motor – reactor shaft lever (3) pressure regulator (4) gas hose (5) HDO reactor (6) product sampling port (7) pressure gauge (8) reactor shaft

Plate 3.3 Gas chromatograph–mass spectrometer (GC–MS)

Since there was technical limitation and difficulty in the online quantification and analysis of the evolved gases (Ŋgas) during the study, they were calculated according to Equation 3.3, and the liquid product distribution was evaluated using Equation 3.4.

$$Ŋgas = [M_b + M_{H2} - M_a] \quad (3.3)$$

$$\omega_i(\%) = \frac{n_i}{\sum_{i=1}^{j} n_i} * 100 \quad (3.4)$$

where M_b is the mass of reactor with the OA and catalyst before reaction, M_{H2} is the mass of total H_2 gas required during the experiment evaluated from the H_2 flow rate and its density. M_a is the mass of the reactor with the liquid product and used catalyst after reaction. Similarly, $\omega_i(\%)$ is the mass fraction of the components in the liquid product.

3.5.2 Qualitative Hydrodeoxygenation (HDO) Experiments and product analysis

Besides the studies of the factors that influence the HDO of MCs, certain studies were undertaken to investigate the HDO process chemistry with reaction time. A high thermal resistant alumina crucible (HTRAC) located in the Thermo-gravimetric analyzer shown in Plate 3.4 (STA 449 F1/F3 with Automatic Sample Changer, Netzsch, Germany) was used as the reactor chamber.

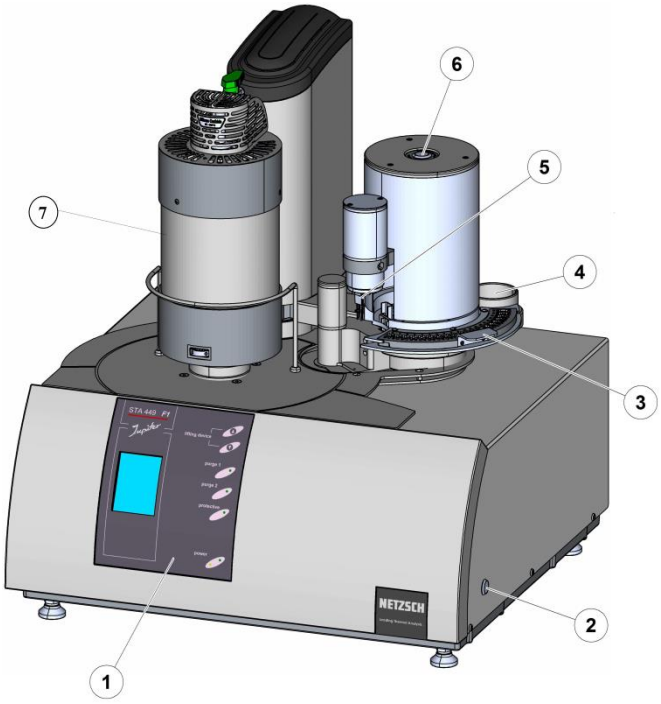

1. Control display (on/off)
2. Safety keys
3. Crucible magazine
4. Gripper guide
5. Gripper
6. Function key (emergency stop)
7. Reactor chamber

Plate 3.4 STA 449 F1/F3 with Automatic Sample Changer (ASC)

The products exit port was coupled to a FTIR spectroscopy instrument (OPUS v7.0, Bruker Optics) shown in Plate 3.5 to concomitantly monitor the rate of MCs disappearance (i.e. rate of reaction) in the presence of understudied catalyst and the qualitative analysis of the evolved products. In a typical catalytic experiment based on

preliminary studies, 3.5 g OA and 2.0 mg of FPdOx/Zeol were carefully premixed in the HTRAC. The mixture was heated at the heating rate of 30 °C/min from 30 to 360 °C, with 20 ml/min of nitrogen flow as protective gas for the HTRAC. After about 10 min when traces of products were noticed from the FTIR display a mixture of high purity H_2/N_2 (5%) at a flowrate of 100 ml/min was continously bubbled into the reactor. The vapors of the reaction product were conveyed into the FTIR instrument via a transfer tube which was kept at 200 °C to maintain the reaction products in the vapor phase for analysis. The analysis of the products spectra was done every 7.03 sec at a spectra resolution of 1 cm^{-1} in the wavenumber range of 4000-600 cm^{-1}. In order to verify that the mass loss recorded by the TG analyzer was strictly due to the HDO of OA and not in conjuction with moisture and volatile matter from PdOx/Zeol , a blank experiment was earlier conducted solely for the thermal gravimetric behavior of FPdOx/Zeol catalyst.

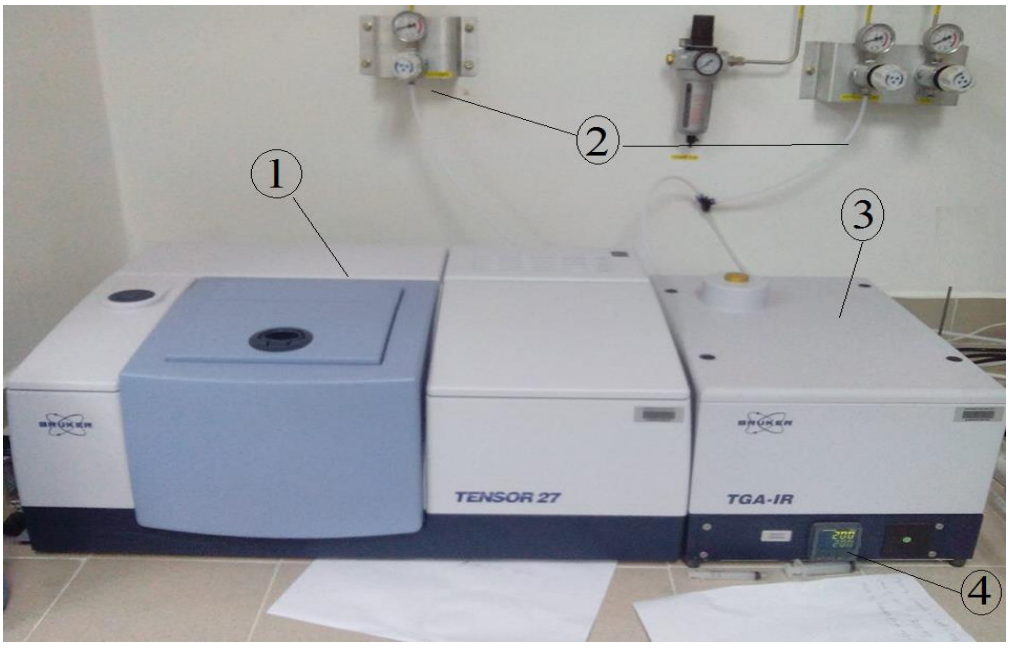

Plate 3.5 FTIR spectroscopy instrument (OPUS v7.0, Bruker Optics). 1. Product sampling zone, 2. Gas supply units, 3. Mild temperature furnance, 4.Furnance temperature display

3.6 Effect of Operating Parameters on the Hydrodeoxygenation Process

3.6.1 Effect of Reaction Time

The effect of reaction was studied over a range of 0 – 60 min because preliminary results and literature studies showed that time has critical effects not only on the process kinetics but it also affects the product distribution as prolong reaction time was observed to be detrimental to the process by producing polymerized and cracked products. During the study, other parameters were fixed as shown in Table 3.2.

3.6.2 Effect of Catalyst Loading

In view of enhanced yield in the target fraction leading to increase HDO process efficiency as the catalyst loading was increased and subsequent reduction in the yield of target fraction with further increase in the catalyst loading, the contributory effect of catalyst loading was studied. The range of catalyst loading was 10, 20, 30 and 40 mg based on preliminary studies. All experiments were carried out at a temperature of 360 ^{o}C, Pressure of 20 bar and gas flow rate of 100 ml/min.

3.6.3 Effect of Temperature

The contributory effects of reaction temperature was investigated in the range of 300 – 380 ºC in some earlier study and in the range of 320 – 380 ºC in subsequent studies since the results showed no scientific contribution and certain research consumables and facilities are limited. The effect of temperature was studied at the best catalyst loading and reaction time.

3.6.4 Effect of Reaction Pressure

The effect of reaction pressure was studied over a range of 10 – 40 bar based on few preliminary runs which were in line with some literature values. The pressure were varied at a reaction condition of 360 ºC temperature, 20 mg catalyst loading and 100 ml/min of gas flow rate.

3.6.5 Effect of Gas Flow Rate

The effect of gas flow rate was also studied over a range of 50 – 150 ml/min to ascertain its contributory and adverse effects on the HDO process. The study was carried out keeping other parameters constant as shown in Table 3.2 of the Experimental Matrix.

Table 3.2 Experimental Matrix*

S/n	Reaction time (min)	Temperature (ºC)	Catalyst Loading (mg)	Gas flow rate (ml/min)	Pressure (bar)
1	60	320	20	100	20
2	60	340	20	100	20
3	60	360	20	100	20
4	60	380	20	100	20
5	60	360	20	100	10
6	60	360	20	100	30
7	60	360	20	100	40
8	15	360	20	100	20
9	30	360	10	100	20
10	45	360	20	100	20
11	60	360	30	50	20
12	60	360	40	150	20

* Applied for 5 different independent studies (totaling 12 x 5 = 60, excluding reusability runs)

3.7 Experimental Matrix

The experimental matrix in Table 3.2 was used as the template for the experimental design for results shown in all the Parts in Chapter Four of the study except Part One, Six and Eight which are devoted to HDO process thermodynamic feasibility studies, HDO process chemistry based on reaction products FTIR studies and process optimization, respectively. The experimental design and matrix for Part Eight – process optimization is shown in Table 3.4 under Section 3.8 below.

3.8 Experimental design and statistical analysis

A four factor D-optimal design was used to determine the optimum operating conditions for maximizing the HDO and ISO of OA into paraffinic biofuel. The four factors selected as independent variables are based on previous and preliminary studies more so the process can be adapted to existing crude oil refinery installations. They are temperature, pressure, catalyst loading and reaction time, and they are assigned with the following notations A, B, C, and D, respectively, their studied range is shown in Table 3.3.

Table 3.3 Table of factors to be optimized using D-Optimal design

Factor	Name	Units	Low Actual	High Actual	Low Coded	High Coded
A	Temperature	ºC	340	380	-1	1
B	Pressure	atm	10	30	-1	1
C	Catalyst	mg	20	40	-1	1

D	Time	min	30	90	-1	1

The objective functions to be optimized are HDO and ISO efficiency and they are denoted as Y and Z, respectively. The number of experiments for the four independent variables was calculated as follows according to DOE configuration using Design-Expert 6.0.6 from Stat Ease Inc.:

Minimum model points	-	15
Lack of fits estimate points	-	5
Replicates points	-	5
Total experiments	-	25

Application of D-optimal design as an optimization technique requires the selections of a model at the beginning, in this particular case study, quadratic model was chosen as shown in Equation (3.5 – 3.6). The adequacy of the final model was verified by graphical and numerical analysis followed by evaluation for the response function and finally the experimental data were analyzed statistically applying analysis of variance (ANOVA).

$$Y = a_0 + a_1A + a_2A + a_3C + a_4D + a_{12}AB + a_{13}AC + a_{14}AD + a_{23}BC + a_{24}BD + a_{34}CD + a_{124}ABD + a_1A^2 + a_2B^2 + a_3C^2 + a_4D^2. \quad (3.5)$$

$$Z = b_0 + b_1A + b_2B + b_3C + b_4D + b_{12}AB + b_{13}AC + b_{14}AD + b_{23}BC + b_{24}BD + b_{34}CD + b_{124}ABD + b_1A^2 + b_2B^2 + a_3C^2 + a_4D^2. \quad (3.6)$$

where a_n and b_n are the coefficients associated with each nth factor, and combination of factors (such as AB) represents interactions between the individual factors in that term.

Table 3.4 Experimental design and response based on experimental runs proposed by D-optimal design

Standard Order	A	B	C	D
1	340	30	20	60
2	340	20	20	90
3	380	30	30	90
4	380	30	20	30
5	340	10	40	30
6	340	30	30	30
7	340	30	40	90
8	380	10	20	90
9	380	30	40	30
10	380	10	40	90
11	340	10	20	30
12	360	30	20	90
13	360	20	40	60
14	340	10	30	90
15	380	10	30	30
16	360	20	25	60
17	340	20	30	60
18	380	20	30	60
19	360	10	30	60
20	360	30	30	60
21	380	10	20	90
22	380	30	20	30
23	340	10	20	30
24	340	30	40	90
25	380	30	40	30

3.9 Kinetics studies of hydrodeoxygenation of oleic acid

In order to study the effect of oxalic acid functionalization on the synthesized supported catalysts, comparisons on the kinetics and Arrhenius parameters of nickel oxalate and nickel oxide supported on alumina catalysts (earlier described in section 3.3.1) was studied on the HDO of the OA. Previous studies (Kovacs et al., 2011; Santillan-Jimenez et al., 2013) have shown that HDO of unsaturated feed stocks such as OA proceeded via sequential hydrogenation to form the saturated SA followed by oxygen molecule extraction to produce the final biofuel (Equation 3.7 – 3.8). This mechanistic step is due to the presence of double bond in the OA structure as shown in Figure 3.1.

$$C_{17}H_{33}COOH + H_2 \rightarrow C_{17}H_{35}COOH \quad (3.7)$$

$$C_{17}H_{35}COOH + 3H_2 \rightarrow C_{18}H_{38} + 2H_2O \quad (3.8)$$

In the HDO of OA, SA was observed to be the main intermediate product, although some other species may be present in varying minute quantity. In order to model a mechanism that can be modestly solved, a lumped kinetic model was adopted as shown in Scheme 3.1, where SA represents all the intermediate compounds since its concentration excessively outweighs that of any other possible intermediate products (Zhang et al., 2013; Ayodele and Togunwa, 2014). Similarly, since the concentration of OA is far in excess of H_2 gas, a pseudo-first-order kinetics was assumed to determine the rate constants, k_i (i = 1, 2, 3) (Zhang et al., 2013; Ayodele and Togunwa, 2014) and also to establish whether the SA formation step or its consumption step is the limiting step. Series of differential equations were obtained from Scheme 3.1 and solved to

arrive at the kinetic model in Equation 3.9 and the experimental data of C_{18} biofuel production at temperature ranges were fitted into it using MathCAD v13.

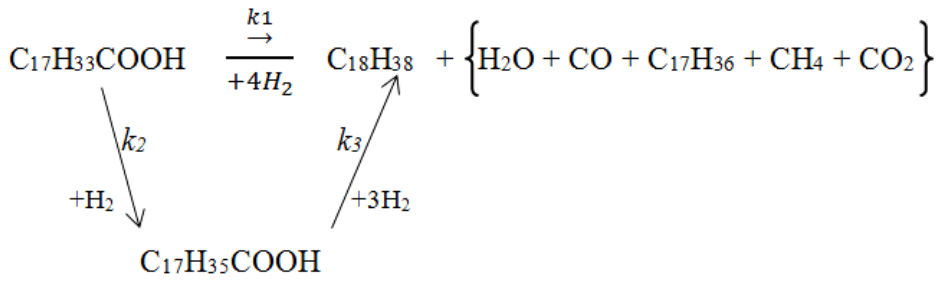

Scheme 3.1 Simplified proposed mechanism for the HDO kinetics of oleic acid

Notation: $C_{17}H_{33}COOH \rightarrow OA$; $C_{17}H_{35}COOH \rightarrow SA$; $C_{18}H_{38} \rightarrow C_{18}$ (biofuel)

$$\frac{C_{18}}{C_{OA_o}} = \frac{1}{(k_3 - k_2)}\left[k_3(1 - e^{-(k_2)t}) - k_2(1 - e^{-(k_3)t})\right] \quad (3.9)$$

3.10 Catalyst Reusability Study

The catalyst reusability study was carried out at the best observed experimental conditions at three to five consecutive cycles. The catalyst was recovered from the reaction after each cycle in a centrifuge, washed with ethanol and dried in the oven at 120 ^{o}C for 12 h. The recovered catalyst was weighed before reuse to determine if the initial weight was consistent after prior use. In all about 18 reusability studies were carried out in this study, i.e. 3 reusability studies per experimental study on each catalyst reported in all the Parts in Chapter Four except Part One and Six.

3.11 Research Activity Diagram

The overall research activity in this study is summarized in Figure 3.4

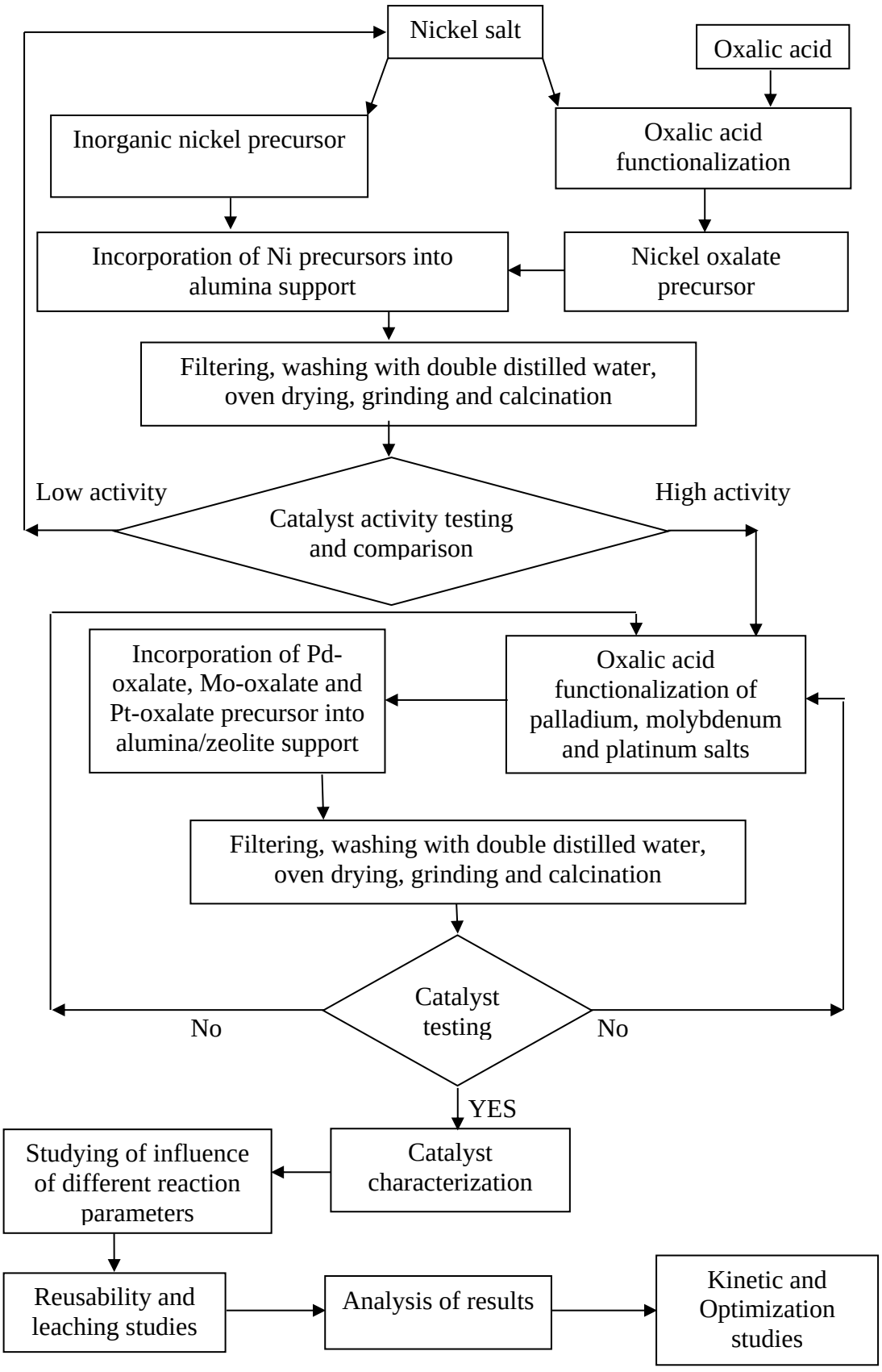

Figure 3.4 Research activity diagram